Animal Biotelemetry

METHODOLOGY

Open Access

Characterization of acoustic detection efficiency using an unmanned surface vessel as a mobile receiver platform

Eric M. Gaskell[1*], Tyler R. Funnell[2], Christopher M. Holbrook[2], Darryl W. Hondorp[3] and Xiaobo Tan[1]

Abstract

Studies involving acoustic telemetry typically use stationary acoustic receivers arranged in an array or grid. Unmanned surface vehicle (USV)-based mobile receivers offer advantages over the latter approach: the USV can be programmed to autonomously carry a receiver to and from target locations, more readily adapting to a survey's spatial scope and scale. This work examines the acoustic detection performance of a low-cost USV developed as a flexible sensing platform. The USV was fitted with an acoustic receiver and operated over multiple waypoints set at increasing distances from the transmitter in two modes: drifting and station-keeping. While drifting, the USV was allowed to drift from the waypoint; while station-keeping, the USV used its thruster to hold position. Detection performance of the USV was similar to that of stationary receivers while drifting, but significantly worse while station-keeping. Noise from the USV thruster was hypothesized as a potential cause of poor detection performance during station-keeping. Detection performance varied with the depth of the tethered receiver such that detection range was greater during the deepest (4.6 m) trials than during shallower (1.1 and 2.9 m) trials. These results provide insight and guidance on how a USV can be best used for acoustic telemetry, namely, navigating to a planned waypoint, drifting and lowering the receiver to a desired depth for listening, and then navigating to the next waypoint.

Background

Acoustic telemetry is a commonly used practice for monitoring fish movement and migration in rivers [1], lakes [2], and oceans [3, 4]. In acoustic telemetry, fish are tagged with acoustic transmitters that broadcast a unique ID code, released back into the environment, and then tracked using acoustic hydrophones or 'receivers'. Acoustic telemetry allows for more frequent observations of individual animals than might be expected using other survey methods (e.g., trawls and gill nets). In most applications, networks of stationary receivers are used to describe individual [5] or population-scale movements [1, 3]. Increasing use of acoustic telemetry arrays has allowed researchers to investigate how aquatic animals interact with their environment in greater detail [6, 7], but has also necessitated a more accurate characterization of its performance [8, 9] as well as an understanding of the limitations and advantages of possible study designs [10]. Although this practice allows for data to be collected continuously at multiple locations, researchers must carefully select receiver locations to avoid introducing unintentional biases in the data, which may be mitigated by applying in situ measures of acoustic array performance [11, 12]. Performance of acoustic telemetry systems also is dependent on environmental conditions (e.g., thermal stratification [13–15], storms [14], surface

*Correspondence:
Eric M. Gaskell
gaskelle@msu.edu
[1] Smart Microsystems Lab, Department of Electrical and Computer Engineering, Michigan State University, East Lansing, MI 48824, USA
[2] U.S. Geological Survey, Hammond Bay Biological Station, 11188 Ray Rd., Millersburg, MI 49759, USA
[3] Great Lakes Science Center, U.S. Geological Survey, 1451 Green Rd., Ann Arbor, MI 48105, USA

water velocity [8], transmitter depth [8], ice presence and thickness [8], aquatic vegetation [1]), many of which vary over time and space.

Mobile telemetry, in which receivers are attached to underwater or surface vehicles, is increasingly being used as an alternative, or complement, to stationary receiver arrays to describe movements and distribution of acoustic-tagged fish. Multiple studies have evaluated factors affecting receiver detection efficiency while attached to mobile platforms, as well as documented the use of mobile telemetry platforms in science and research [16–19]. Distance, water depth, and wind speed were found to be the most significant factors affecting the performance of mobile telemetry systems. Detection probability was found to decrease with increasing wind speed and distance, and was found to increase with increasing water depth [16]. Unmanned surface vehicles (USVs), also known as autonomous surface vehicles (ASVs), and autonomous underwater vehicles (AUVs) are able to carry an acoustic receiver as either a self-contained payload or as an integrated sensor. Saildrones (Saildrone Inc., Alameda, CA, USA), a type of USV powered by solar and wind, were used to quantify the spatial distribution of fishes in the Bering Sea [19]. REMUS-100 (Woods Hole Oceanographic Institute, Woods Hole, MA, USA) propelled AUVs were used to autonomously follow acoustically tagged basking sharks and to monitor tagged sturgeon in their spawning habitat [20, 21]. Wave gliders (Boeing—Liquid Robotics, Herdon, VA, USA) (a type of AUV that move using wave energy collected by a tethered float) [18] and buoyancy-driven underwater gliders [16, 22, 23] are other examples of technologies that have been used as mobile acoustic telemetry platforms. Lastly, gliding robotic fish (e.g., GRACE, MSU Smart Microsystems Laboratory, East Lansing, MI, USA) [24–28], another form of buoyancy-driven AUV similar to gliders, were also explored as a mobile telemetry platform. For gliding robotic fish, detection efficiency was higher when the hydrophone was pointed toward the transmitter, and lower when it was pointed away. When selecting a mobile platform for acoustic telemetry, there are many important factors to consider including experiment design, environment, spatial scale and cost. Propeller-driven AUVs (e.g., REMUS-100, and Iver2, L3Harris OceanServer, Fall River, MA, USA) generate more thrust than other platforms, but consume more power [20, 21, 29]. Such AUVs may be more suitable for experiments in high current over relatively short time frames and smaller spatial scales. Robotic Sailboats (e.g., Saildrone,) and buoyancy-driven AUVs (e.g., Slocum G3, Teledyne Marine, Webb Research, North Falmouth, MA, USA) are more power-efficient, but may not be suitable for higher currents [16, 17, 19, 22, 23, 30]. Due to the relatively short distance radio waves can travel through water, AUVs cannot communicate using RF signals unless they are at the surface [31, 32]. This limits their ability to localize with RF-based position sensors such as GPS, making them less suitable for studies that require precise localization. Although such AUVs have been explored as mobile telemetry platforms, they are not commonly used due to their high cost.

This paper examines performance of a low-cost, easy-to-manufacture USV as a potential acoustic telemetry platform (dubbed CHASE, for Catamaran-Hulled Autonomous Surface Experimental platform). CHASE can be pre-programmed with a mission plan using third-party software or driven manually, and can be fitted with a variety of sensors. CHASE is intended to be an accessible platform for use by non-experts, being constructed from off-the-shelf components at a lower cost than other USVs, and operated through a third party supported user interface. In this study, detection efficiency is estimated and compared between the CHASE platform and a line of stationary receivers. The effects of operating mode (drifting or station-keeping), thruster use, receiver depth, and receiver configuration on detection performance are investigated. This characterization of the CHASE platform is intended to lay the groundwork for future research into waypoint selection and using USVs for localizing and tracking tagged fish.

Methods

CHASE USV platform

The CHASE USV (Smart Microsystems Laboratory, Michigan State University, East Lansing, MI, USA), shown in Fig. 1, is a flexible experimental platform developed to be refitted with different sensors. CHASE is designed to be a low-cost, easy-to-manufacture sensing platform constructed with mostly off-the-shelf components. An acoustic receiver, either integrated or independent of the CHASE system, can be attached. We conducted tests using an independent VEMCO VR2Tx receiver (Halifax, NS, Canada) attached via a paracord tether with the hydrophone oriented down. We also tested an alternative configuration with a receiver (VEMCO miniVR2C, Halifax, NS, Canada) wired into an integrated sensor hub, which allowed remote access to acoustic telemetry data over a Wi-Fi network in real time. For both configurations, a 3.63 kg lead weight was positioned 0.5 m above the receiver to maintain vertical orientation of the tether. The sensor hub communicated with the receiver using a Raspberry Pi 3B (Raspberry Pi Foundation, Cambridge, England), and networked with a Wi-Fi router (Linksys, Irvine, CA, USA) at the surface using a kevlar-reinforced ethernet cable. CHASE was controlled by a PixHawk 2.4.8 (Multiple manufacturers)

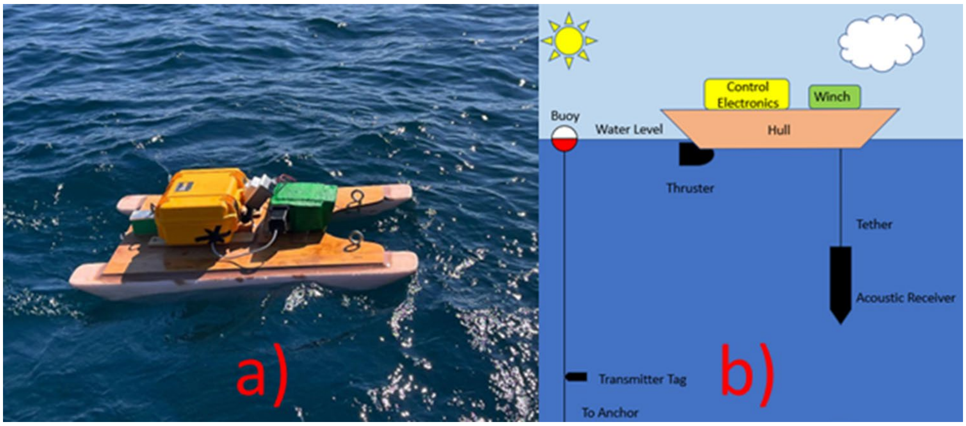

Fig. 1 **a** Unmanned surface vehicle CHASE with acoustic receiver on a network tether, photograph by Xiaobo Tan, Michigan State Univeristy (VEMCO mini VR2C); **b** diagram of experimental setup for CHASE mobile detection efficiency tests showing USV platform, receiver (VEMCO mini VR2C or VEMCO VR2Tx), and test transmitter. Not to scale

running ArduRover 4.2.2 firmware, and QGroundControl software (version development HEAD:78cf9bbe6 2021-05-06 10:49:59 -0700, San Francisco, CA, USA) on a ground control computer was used for vehicle navigation control. Geographic location of the vehicle was determined from a M8N GPS sensor (U-Blox, Thalwil, Switzerland), which was integrated with the PixHawk's internal IMU (Inertial Measurement Unit) in a Kalman filter to produce an accurate estimate of position and orientation. Prerecorded mission files specifying waypoints and loiter duration were loaded onto the USV from the ground control computer. Position and orientation information was sent over 915 MHz radio to the ground control computer at a nominal rate of 1 Hz. CHASE's twin hulls were made from resin-covered foam insulation, and vehicle deck was constructed of a single piece of resin-covered plywood. The vehicle was powered by a T-200 thruster (Blue Robotics, Torrance, CA, USA), and steering was accomplished using a servo motor to turn the thruster. Due to the relatively small (1 m length) and light nature of the CHASE USV, thrust was limited to 50 percent at maximum. Operating at 50 percent of the maximum thrust was found to be sufficient for navigation and station-keeping, whereas operating at higher thrusts reduced vehicle stability.

Study area

The study area was chosen in Hammond Bay, an oligotrophic embayment of Lake Huron, in a location with little boat traffic and relatively flat bathymetry. This area was far enough away from other ongoing acoustic telemetry studies in Lake Huron to avoid interference from acoustic-tagged fish. Local temperature and wind speed data were recorded by the KMIMILLE10 weather station in Millersburg, MI over the duration of the study (Table 1).

Stationary receiver tests

An acoustic transmitter (V13-1x, Innovasea, Halifax, NS, Canada) was suspended 6.1 m off bottom at a site where bottom depth was 22.6 m (Fig. 2). Transmissions were broadcast at 69 kHz in alternating low- and

Table 1 Description of operating mode, tether length, acoustic receiver used, and weather conditions for each trial [42].

Trial number	Mode	Tether length	Receiver	Date	Duration	Weather conditions
1	Station-Keeping	4.6 m	VR2TX	8/17/2022	1:56	21.1 °C, 1.7 m/s wind
2	Drifting	4.6 m	VR2TX	8/18/2022	1:54	13.8 °C, 1.2 m/s wind
3	Drifting	2.9 m	VR2TX	8/18/2022	1:44	15.6 °C, 0.9 m/s wind
4	Station-Keeping	2.9 m	VR2TX	8/18/2022	1:24	23 °C, 0 m/s wind
5	Drifting	2.9 m	VR2TX	8/19/2022	1:20	16.1 °C, 0 m/s wind
6	Drifting	1.1 m	VR2TX	8/19/2022	1:37	15.7 °C, 0.4 m/s wind
7	Station-Keeping	1.1 m	VR2TX	8/19/2022	1:38	18.9 °C, 0.6 m/s wind
8	Drifting	2.9 m	Mini VR2C	8/19/2022	1:54	24.5 °C, 0.4 m/s wind

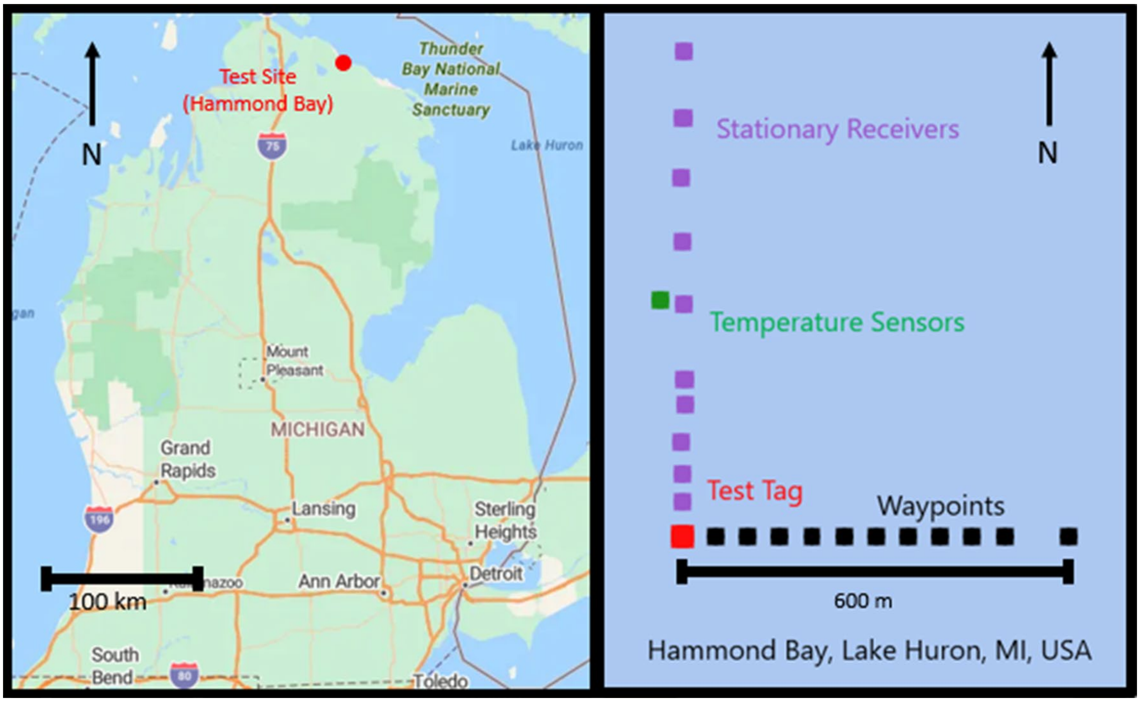

Fig. 2 (Left) Location of Hammond Bay, Lake Huron. (Right) Locations of test transmitter tag, stationary receivers and USV waypoints (approximately 1 km). Microsoft Excel software (Microsoft, Redmond, WA, USA) was used to generate map images

high-power (low power output = 147 dB re 1 µPa @ 1 m; high power output = 152 dB re 1 µPa @ 1 m) with each power setting uniquely coded. Transmissions occurred at a nominal delay of 60 s, resulting in uniformly distributed random intervals from 34 to 94 s, assuming a 4-s burst duration for each transmission. Due to the alternating nature of the transmissions, intervals between unique codes were assumed to be 68 to 128 s. For comparison with the mobile telemetry platform, ten VEMCO VR2AR (Halifax, NS, Canada) stationary receivers were placed in a line extending north from the transmitter at approximate distances of 50 m, 100 m, 150 m, 200 m, 250 m, 350 m, 450 m, 550 m, 650 m, and 750 m from the transmitter (Fig. 2) at bottom depths ranging 22.9–27.1 m (mean = 24.9 m). Receivers were suspended with floats 3 m off the lake bottom (resulting depth of receivers in the water column: range = 19.9–24.1 m) with the hydrophone up, which is a standard receiver mooring arrangement in the Great Lakes. Stationary receivers recorded any transmissions from the test transmitter that were successfully received for the duration of the mobile detection efficiency tests, to provide an in situ measure of baseline receiver detection efficiency.

Mobile detection efficiency tests

Several detection efficiency trials were conducted using the CHASE USV to quantify overall detection efficiency and to determine if detection efficiency was affected by (1) operating mode (drifting vs. station-keeping); (2) instantaneous use of the thruster (on vs. off); (3) tether length; and (4) receiver integration (integrated sensor hub vs. independent tether). Initial pilot runs revealed a relatively low detection probability using the integrated sensor hub, so seven of the eight trials were conducted using an independent VEMCO VR2Tx acoustic receiver on a paracord tether. Detections were recorded for the entire trial, including during travel between waypoints and time spent loitering at waypoints. The seven trials conducted with the independent receiver were used to evaluate effects of operating mode (drifting vs. station-keeping), thruster condition, and tether length. In drifting mode, the USV was driven to each waypoint and allowed to drift freely for 5 min before moving to the next waypoint. The median distance that the USV drifted from the waypoint across all trials was found to be 40.3 m, while the maximum distance that the USV drifted was found to be 73 m. In station-keeping mode, autonomous control was used to visit each waypoint for 5 min during which the thruster held position within 2.14 m of the waypoint, the minimum value allowed by the firmware. While station-keeping, the thruster was used only when needed and instantaneous use of the thruster at the time of each transmission was recorded. Waypoints were spaced at 50-m intervals, beginning at the transmitter and extending eastward to a distance of 500 m, with one final waypoint at a distance of 600 m from the transmitter (Fig. 2). Initial trials extended further than this distance, but later trials were shortened due to poor performance beyond 600 m. Waypoints were chosen to the east of the transmitter to avoid potential collisions with stationary receiver buoys to the north of the transmitter. We make the assumption that direction of waypoints from the transmitter would not have a meaningful influence on detection probability given that lake bathymetry was relatively flat and uniform over the study area and that elevation of all instruments above the lake bottom ensured line of sight, regardless of direction from the transmitter. Positive detections beyond 650 m were rare (1 detection of 118 transmissions); therefore, data from USV runs were filtered to include transmissions only when the USV was within 650 m of the transmitter. Trials in each operating mode were conducted at tether lengths of 1.1 m (short), 2.9 m (medium), and 4.6 m (long). All combinations of operating mode and tether length were tested with a duplicate of the test of drifting mode at the medium tether length for a total of seven trials using the VR2Tx. The test of drifting mode at medium tether length was repeated to ensure consistency after a storm occurred. An eighth trial was conducted with a receiver (VEMCO miniVR2C) connected to an underwater sensor hub in drifting mode at the medium tether length. For a description of each trial conducted, see Table 1.

Temperature profile

To determine if thermal stratification of the water column affected comparisons of detection performance between stationary and vehicle-mounted receivers, seven temperature sensors (Onset Hobo Water Temp Pro V2, Bourne, MA, USA) affixed to an anchored line about 370 m north of the test transmitter location in 25.0 m water depth recorded the temperature in the water column for the duration of the experiments. Water column temperature was monitored at a single station (Fig. 2) with loggers deployed at depths of 3.6 m, 6.9 m, 10 m, 13.3 m, 16.7 m, 19.9 m, and 23.3 m, below the surface. Loggers were deployed about 3 days prior to the first trial and were retrieved after about 8 days, after all trials had been conducted. Strength of stratification was quantified as the temperature gradient (°C/m) between 16.7 m (i.e., the logger at the water depth nearest the transmitter) and 3.6 m for the mobile receiver and 23.3 m for the stationary receivers, averaged for each trial.

Data analysis

Detection efficiency was quantified by assigning each transmission as a success or failure (i.e., missed detection) at each receiver. Every transmission during each trial was assumed to be heard by at least one receiver based on standardization of detections across all stationary receivers. Detections were standardized by applying a linear time correction to the data collected by all receivers using VDAT software (Innovasea), then applying a pattern-matching algorithm that uses the unique sequence of random delays from the transmitter by treating the receiver closest to the transmitter as the reference clock. Following standardization, time between detections was always between 33 and 94 s, suggesting that all transmissions were detected by at least one receiver. Resulting data were binomial (0: failure, 1: success) and were filtered to include only detection data during USV trials. All data collected by the mobile receiver within 650 m of the transmitter (i.e., regardless of whether the USV was at a waypoint or in transit) were included in analyses, unless otherwise specified below. High- and low-power transmissions were modeled independently in all subsequently described analyses.

Operating mode and stationary receiver comparison

We first compared overall detection efficiency of stationary receivers to USV trials in each operating mode, drifting and station-keeping, with the tethered receiver. Detection probability curves were constructed using a generalized additive mixed model (GAMM) with a binomial error structure (model 1). The effect of USV operating mode or stationary receivers on detection range curves was evaluated in model 1. Detection probability was modeled as a function of operating mode (i.e., drifting or station-keeping modes of the USV, or stationary receivers), a smoothed function of distance, a smoothed function of distance for each mode, a random effect of trial, and a random effect of trial by distance. Random effects relating to trial were included to account for environmentally influenced differences in detection efficiency that would have been reflected in the mobile and stationary receivers during a trial.

Effects of thruster and tether length

The effects of two potential explanatory covariates on detection efficiency were evaluated using a generalized additive model (GAM) with a binomial error structure (model 2). Detection probability from USV trials only (i.e., excluding stationary receivers) was modeled as a function of operating mode, tether length, instantaneous thruster use at the time of transmission, a smoothed function of distance, a smoothed function of distance for each mode, a smoothed function of distance for each tether length, and a smoothed function of distance for each thruster status. Tether length was treated as a factor with values of short (1.1 m), medium (2.9 m), and long (4.6 m). Thruster was treated as a binary factor, either off

(0) or on at any thruster level (1), taken from the time of transmission/detection.

Effect of mobile receiver integration

Detection performance of the integrated sensor hub was compared to performance in analogous trials with the tethered receiver using a GAM with a binomial error structure (model 3). Only data from trials in drifting mode with the medium tether length were used for model 3, which included two trials with the tethered receiver and one trial with the sensor hub (Table 1). Additionally, data were filtered to only consider transmissions when the USV thruster was off, as no positive detections were recorded when the USV thruster was on in these trials. Detection probability from filtered trials was modeled as a function of receiver type (tethered VR2Tx or sensor hub mini VR2C), a smoothed function of distance, and a smoothed function of distance by receiver type.

In all three models described above, the basis for smoothed functions was a cubic regression spline with shrinkage and 5 knots. The use of a smoothed function with shrinkage allowed non-meaningful parameters to be reduced in their effective degrees of freedom to a value as small as zero [33], thereby effectively excluding these parameters without the need for hierarchical model selection. All models were fit using restricted maximum likelihood with the "gam" function from the "mgcv" library [34] in R 4.2.2 [35].

Results

Operating mode and stationary receiver comparison

Detection efficiency of the mobile receiver attached to the CHASE USV was similar to or lower than that of stationary receivers at most distances and configurations. Detection probability for stationary receivers was greater than 95% up to 250 m from the transmitter for high-power transmissions and up to 200 m from the transmitter for low-power transmissions, and decreased with increasing distance from the transmitter after these points (Fig. 3). Conversely, detection probability of the mobile receiver followed a concave-shaped curve with distance, i.e., detection probability peaked at an intermediate distance from the transmitter, under both operating modes (Fig. 3). Detection performance of the mobile receiver was substantially lower in station-keeping mode compared to the mobile receiver in drifting mode and the stationary receivers at all distances for both high- and low-power transmissions (Fig. 3). In drifting mode, overall mobile receiver performance was similar to that of stationary receivers at distances between roughly 250 and 500 m from the transmitter for high-power transmissions and greater than 250 m from the transmitter for low-power transmissions (Fig. 3). Mobile receiver detection performance in drifting mode was lower than stationary receiver performance at distances close (i.e., < 250 m) to the transmitter for high- and low-power transmissions and at distances far (i.e., > 500 m) from the transmitter for high-power transmissions (Fig. 3).

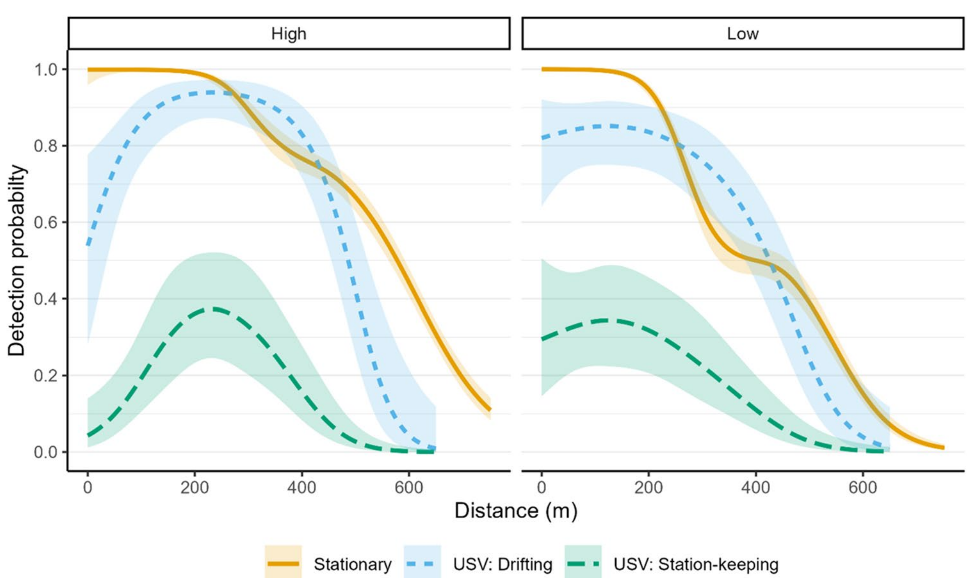

Fig. 3 Detection range curves for high- (left) and low-power (right) transmissions. Lines represent GAM outputs for stationary receivers (solid orange) and the mobile receiver trials in drifting mode (small-dashed blue) and station-keeping mode (large-dashed green). Shaded regions are 95% confidence intervals of model predictions

Effects of thruster and tether length

Detection probability of the mobile receiver was dependent on several covariates including operating mode, thruster, and tether length. When accounting for thruster and tether length, detection probability for high-power transmissions followed a concave curve with detection probability peaking around 210 m from the transmitter (Figs. 4a, 5). Detection probability for low-power transmissions generally followed a decreasing logistic-style curve, characterized by stable detection probability followed by decreasing probability with increasing distance from the transmitter (Figs. 4b, 5). Detection probability was higher in drifting mode than in station-keeping mode for high- and low-power transmissions (Table 2). High- and low-power detection efficiency was lower when the thruster was on compared to when it was off (Table 2). For high-power transmissions, overall detection probability was 0 and 3% in drifting and station-keeping modes, respectively, when the thruster was on compared to 78% and 50%, respectively, when the thruster was off. Similarly, for low-power transmissions, overall detection probability was 0 and 11% in drifting and station-keeping modes, respectively, when the thruster was on compared to 70% and 37%, respectively, when the thruster was off.

Length of the tether attached to the mobile receiver (i.e., depth of the receiver) influenced detection probability, such that the long tether length resulted in slightly longer detection range than the short and medium tether lengths (Fig. 5). Model 2 suggested the long tether length had a significant positive interaction with distance on detection efficiency of high-power transmissions (Fig. 4c), resulting in a detection range curve extending further from the transmitter (Fig. 5, Table 2). Considering drifting mode with the thruster off, the

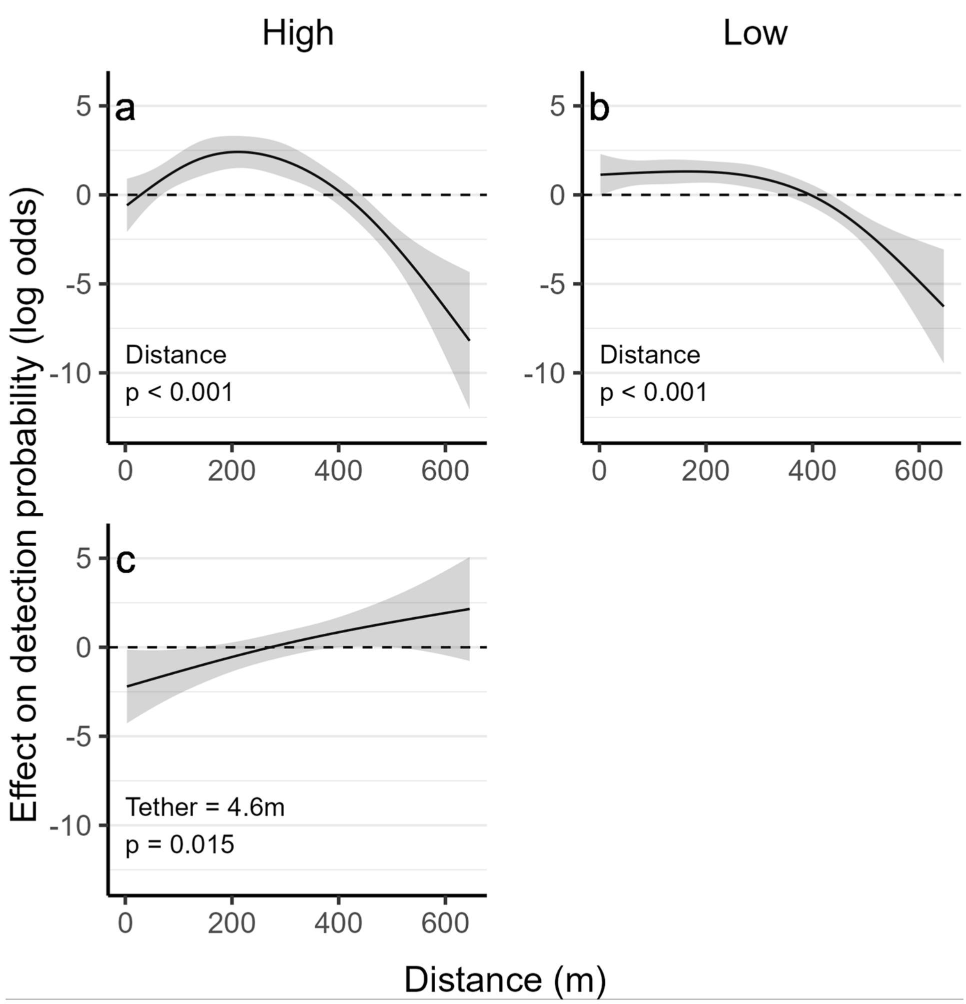

Fig. 4 Partial effects of significant smoother functions on detection probability identified by the GAM considering thruster use and tether length. The left column depicts significant smooths for high-power transmissions: **a** distance and **c** tether length of 4.6 m as a function of distance. The right plot depicts the only significant smooth function for low-power transmissions, **b** distance. *P*-values are given for each effect (see Table 2). Shaded regions are 95% confidence intervals of model predictions

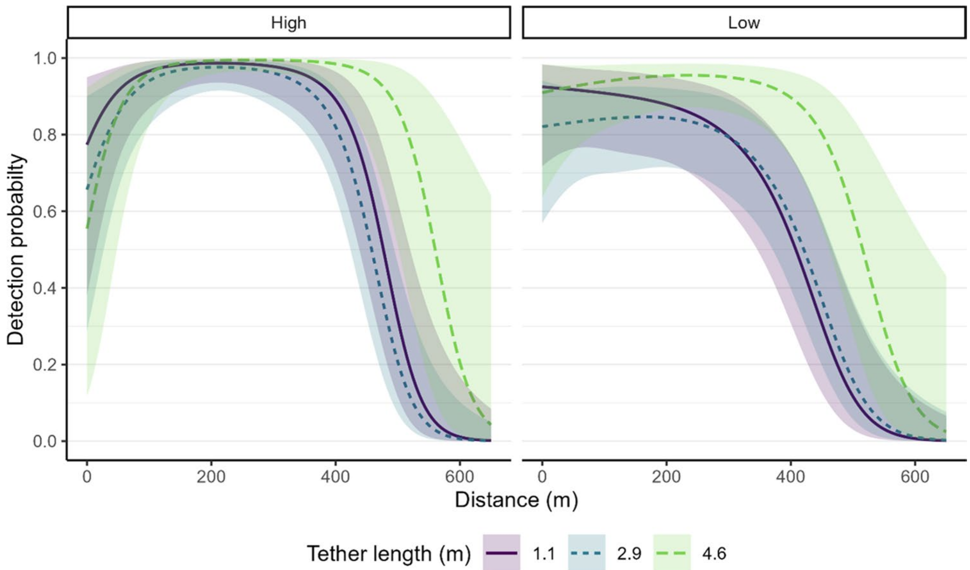

Fig. 5 Detection range curves of USV trials conducted in drifting mode with the tethered receiver (VR2Tx) when the thruster was off. Lines are model predictions at 3 tether lengths (i.e., receiver depth; 1.1 m: solid purple, 2.9 m: small-dashed blue, 4.6 m: large-dashed green) for high- (left) and low-power (right) transmissions. Shaded regions are 95% confidence intervals of model predictions

50% detection probability from the high-power range curve was 83.3 and 102.2 m further from the transmitter for the long tether compared to the short and medium tether lengths, respectively (Fig. 5). For low-power transmissions, the long tether length had a significantly higher detection probability than the short [estimate ± se, log(odds) = 1.37 ± 0.56, *Z*-value = − 2.47, *p*-value = 0.014] and medium tethers [estimate ± se, log(odds) = 1.52 ± 0.52, *Z*-value = − 2.95, *p*-value = 0.003], regardless of distance (Fig. 5, Table 2). Detection range curves for the short and medium tethers were similar with overlapping confidence intervals for high- and low-power transmissions (Fig. 5, Table 2).

Effect of mobile receiver integration

The tethered receiver had generally better performance than the integrated sensor hub. Detection efficiency was higher for the tethered receiver than for the sensor hub (effect of tethered receiver: high-power = 3.94 ± 1.39 [estimate ± se, log (odds)], *p* = 0.005; low-power: 4.88 ± 2.07; *p* = 0.018). For high- and low-power transmissions, the tethered receiver had a higher probability of a positive detection than the sensor hub at distances greater than 40 m from the transmitter (Fig. 6). While confidence intervals were wide due to small sample size in this model, confidence intervals were non-overlapping between 125 and 440 m for high-power transmissions and between 120 and 395 m for low-power transmissions (Fig. 6).

Temperature

Strength of stratification was similar across all trials and was weak (i.e., < 1 °C/m) overall. Average temperature per trial ranged 14.7–17.4 °C (mean = 16.4 °C) near the transmitter, 20.2–20.9 °C (mean = 20.6 °C) near the mobile receiver, and 8.4–12.9 °C (mean = 10.0 °C) near the deepest stationary receiver. The temperature gradient from the transmitter to the mobile receiver ranged from − 0.43 to − 0.21 °C/m (mean = − 0.32 °C/m) while the temperature gradient from the transmitter to the deepest stationary receivers ranged from 0.28 to 0.62 °C/m (mean = 0.49 °C/m) during trials. Temperature gradient recorded during trials was similar to the average gradient during the approximately 8-day period the temperature loggers were deployed (transmitter to mobile receivers = − 0.27 °C/m; transmitter to the deepest stationary receiver = 0.51 °C/m) (Additional file 1).

Discussion

The detection performance in the drifting mode relative to the performance of nearby stationary receivers demonstrate the potential promise of USVs as mobile telemetry platform. Drifting buoys have been explored as a potential acoustic telemetry platform in lakes, where they were found to cover more area and detect more tagged fish than stationary receivers [36]. In drifting mode, USV-based telemetry platforms have the potential to survey more area than the same number of stationary receivers, without the need to deploy and retrieve receivers and without sacrificing detection efficiency. We hypothesized

Table 2 Summary table of parametric coefficients and smooth terms for Model 2, GAMs testing the effect of operating mode, tether length, thruster, a smoothed function of distance, a smoothed function of distance for each mode, a smoothed function of distance for each tether length, and a smoothed function of distance for each thruster status on detection probability of high- (top) and low-power (bottom) transmissions

Parametric coefficients	Estimate	SE	Z	*p*-value
High-power				
(Intercept)	1.88	0.57	3.30	*9.51E–04*
Mode = Station-keeping	− 2.25	0.62	− 3.65	*2.59E–04*
Tether = 2.9 m	− 0.58	0.60	− 0.96	0.335
Tether = 4.6 m	1.22	0.76	1.60	0.110
Thruster = on	− 5.27	0.91	− 5.78	*7.26E–09*
Smoothing terms	**EDF**		**X^2**	***p*-value**
S (distance)	3.00		33.93	*< 2E–16*
S (distance): mode = Drifting	1.23E–05		1.08E–06	0.823
S (distance): mode = Station-keeping	1.21E–05		1.27E–06	0.795
S (distance): tether = 1.1 m	3.15E–06		8.97E–08	0.945
S (distance): tether = 2.9 m	2.72E–06		1.66E–07	0.880
S (distance): tether = 4.6 m	1.05		4.97	*0.015*
S (distance): thruster = off	2.58E–03		2.52E–03	0.259
S (distance): thruster = on	9.58E–02		0.11	0.284
Parametric coefficients	**Estimate**	**SE**	***Z***	***p*-value**
Low-power				
(Intercept)	0.54	0.42	1.29	0.199
Mode = Station-keeping	− 1.41	0.44	− 3.20	*0.001*
Tether = 2.9 m	− 0.15	0.45	− 0.32	0.746
Tether = 4.6 m	1.37	0.56	2.47	*0.014*
Thruster = on	− 2.91	0.54	− 5.43	*5.54E–08*
Smoothing terms	**EDF**		**X^2**	***p*-value**
S (distance)	2.74		25.75	*5.62E-07*
S (distance): mode = Drifting	1.43E–05		5.56E–06	0.545
S (distance): mode = Station-keeping	1.28E–05		5.81E–06	0.509
S (distance): tether = 1.1 m	0.75		1.65	0.117
S (distance): tether = 2.9 m	3.12E–05		7.49E–06	0.566
S (distance): tether = 4.6 m	0.64		1.35	0.125
S (distance): thruster = off	1.24E–05		7.35E–06	0.432
S (distance): thruster = on	2.17E–05		1.21E–05	0.456

For each model (high- (top) and low-power (bottom) transmissions), parametric coefficients are provided with the estimate, standard error (SE), test statistic (*Z*), and *p*-value for the null hypothesis that the parameter is zero and smoothing terms are provided with the estimated degrees of freedom (EDF), test statistic ($\chi 2$), and approximate *p*-value for the null hypothesis that the smoothing term is zero. Italicized p-values are significant at a significance level of 0.05, see Fig. 5 for the partial effects plots of significant smoothing terms

that the poor detection probability of CHASE in station-keeping mode was caused by noise from the thruster or from water moving over the hydrophone (i.e., hydrodynamic noise). Thrusters are integral to many potential mobile telemetry platforms and, thus, optimization of AUVs/USVs as telemetry platforms will require strategies for minimizing or masking noise from thrusters and/or motors. While detection efficiency suffered when the thruster was on at the time of transmission, thruster status alone did not completely explain the poorer detection performance in station-keeping mode compared to drifting mode. However, thruster status was taken at the time of detection, recorded at a resolution of one second at the end of the 3–4 s burst time of the transmission. Therefore, the thruster could have been activated but unaccounted for during the burst time, which could prevent the acoustic receiver from decoding the entire transmission. Hydrodynamic noise is known to

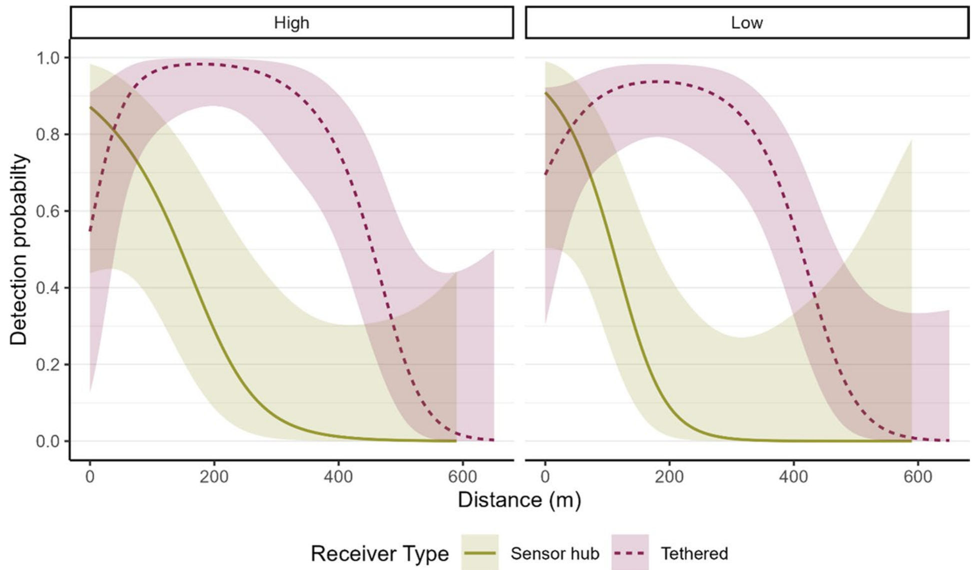

Fig. 6 Detection range curves of USV trials in drifting mode with a tether length (i.e., receiver depth) of 2.9 m when the thruster was off. Lines are model predictions from trials with a tethered receiver (VEMCO VR2Tx; dashed maroon) or integrated sensor hub (VEMCO miniVR2C/RXlive; solid beige) for high- (left) and low-power (right) transmissions. Shaded regions are 95% confidence intervals of model predictions

affect stationary acoustic receiver performance in environments with pronounced flows [37], and, similarly, is expected to affect any aquatic vehicle under active propulsion. Although thruster-driven USVs are not immune to either of these noise sources, their ability to move quickly over the water surface, track their position, and navigate with precision makes them uniquely suited to grid-style telemetry surveys in which both of those noise sources are minimized during discrete listening intervals (i.e., the drifting mode tested here). Although receivers performed poorly during station-holding, hardware or software improvements could minimize the effects of thruster and hydrodynamic noise so that station-keeping mode could be useful during adverse weather conditions or for experiments requiring more precise localization of the acoustic receiver than what the drifting mode can provide.

Detection probability of the mobile receivers was low at distances near the transmitter and peaked at an intermediate distance, which could be indicative of close proximity detection interference, also termed the “doughnut-effect” [38]. Close proximity detection interference can be caused by echoes of a transmission reflecting off hard surfaces, such as rocky substrate or the lake surface, which are detected before the next transmission in a pulse train (i.e., transmission burst), causing failed or misinterpreted detections [38, 39]. To minimize detection of echoes, the types of receivers used in this study stop listening for 260 ms (blanking interval) after detection of each pulse. Thus, close proximity detection interference can only occur when (1) the reflective surface causing the echo is far enough away from the receiver and/or transmitter that the echo arrives at the receiver after the blanking interval and (2) the echo arrives at the receiver with sufficient strength to be detected. This type of detection interference is typically most severe for higher power transmissions [8, 38, 39], as is seen in the present study. However, stationary receivers did not experience close proximity detection interference, suggesting that close proximity detection interference is more prevalent near the surface than the bottom in environments like our study site. We hypothesize that prevalence of echoes from distant objects is positively associated with receiver height off bottom because the amount of substrate in “sight” of a receiver increases with elevation. Transmitters and receivers could be placed at variable depths spanning the water column to investigate critical depths that create, or avoid, conditions that support this detection interference. If our hypothesis is supported, then receiver depth may be modified (via tether length) to minimize close proximity detection interference in certain environments.

Over the range of tether lengths used in this study (1.1–4.6 m), the lower detection range observed for the medium and short tether lengths could be attributed to proximity to the lake surface. Conditions of the lake surface can decrease acoustic detection efficiency through air entrainment resulting from wind and wave action [40, 41]. Interactions between the lake surface and the USV may produce additional noise that could decrease detection efficiency, even when the USV is motionless. Additionally, temperature differences near the lake surface that we were unable to record at a fine enough resolution could contribute to tether length differences in detection range as temperature gradients can negatively impact detection efficiency [13–15]. Weather conditions were ideal during the study period, with low wind speeds, waves typically less than 1 ft, and little thermal stratification. Temporal studies performed when weather conditions are degraded could reveal the effects of wind and thermal stratification on mobile detection performance under a wider range of conditions. In addition, longer tether lengths than were used in this study could aid in determining optimal lengths that maximize detection efficiency and range in different water depths and conditions. Examining the impact of different encoding schemes, as close proximity detection interference is thought to be unique to the PPM encoding scheme, could inform study design to avoid such an effect.

Ideally, a USV-based mobile telemetry platform would allow real-time access to data from the acoustic receiver and other sensors (e.g., temperature). Therefore, an integrated receiver like the mini VR2C should be desired over an electrically isolated VR2Tx. We speculate that poor performance of the mini VR2C receiver connected via sensor hub was caused by electromagnetic or acoustic noise produced by the sensor hub. Such noise may have interfered with detections, but further testing is needed to establish the cause of the poor performance. If the issues with the sensor hub or mini VR2C can be resolved, then further integration of the mini VR2C receiver with the USV may allow operational parameters to be changed in response to in situ environmental conditions (e.g., thermocline) or feedback (e.g., test transmitter detections).

Although USVs have advantages over stationary receivers, they also have several limitations. The spatial and time scales of the study will be limited by battery capacity and accessibility of the vehicle for servicing. For a given duration (e.g., battery life), increasing spatial scale may require allocating more time to moving among waypoints, during which detection efficiency will be poorer than when the USV is not moving. USV-based telemetry platforms may also be more likely to be lost or damaged during a survey, although such losses may be more readily detected and mitigated in mobile platforms than in stationary arrays. Finally, a critical assumption underlying the development of mobile receiver platforms is that stationary receivers are best suited to detection of highly mobile animals (or time periods when animals are highly mobile) and that mobile receivers are best suited to detection of animals with limited mobility (or periods of time when mobility is limited). Due to periodicity in mobility within the life cycle of many organisms and variety of questions that telemetry can be used to address, we expect mobile telemetry to most often complement, rather than replace, stationary telemetry methods.

Conclusion

Detection efficiency of an acoustic telemetry receiver affixed to the CHASE USV was maximized, and most similar to stationary acoustic receivers, when (1) the USV passively drifted (vs. active station-holding) while sampling at each waypoint; (2) an electrically isolated (VR2Tx) receiver was used (vs. a cabled mini VR2C receiver connected via a communications hub); and (3) the receiver was suspended on a 4.6 m (vs. 1.1 m or 2.9 m) tether. Thus, fundamental design elements (e.g., receiver type; attachment method) and operational parameters (e.g., operating mode, and depth of receiver) can have substantial consequences to the efficacy of USV-mounted receivers. Although performance of USV-mounted receivers was similar to stationary receivers under certain conditions (e.g., in drifting mode with a VR2Tx receiver suspended on a 4.6 m tether), this work also identified processes (e.g., close proximity detection interference) and factors (e.g., receiver depth) that are poorly understood, yet could inform changes to further improve performance. Specifically, optimization of USV-mounted receiver platforms would further benefit from understanding: (1) if lower detection efficiencies while station-keeping than while drifting were caused by interference from the thruster or hydraulic turbulence; (2) if poor performance of a cabled mini VR2C receiver connected via sensor hub was caused by acoustic or electromagnetic interference; (3) if higher detection efficiencies with the longest tethers used in this study were related to isolation from surface noise; and (4) if tether lengths longer than those used in this study could further improve detection performance by reducing close proximity detection interference or by mitigating effects of other environmental factors (e.g., thermal stratification; weather-related noise).

Overall, the performance of the CHASE USV in drifting mode makes it a promising platform for telemetry experiments. Mobile platforms may increase the study area and decrease the labor required for a study without significantly sacrificing performance. Better characterizing the effects of transmitter depth and tether length, examining the problem of waypoint selection, and finalizing the design of the USV before disseminating plans for its construction could improve the performance of the CHASE USV.

Supplementary Information

The online version contains supplementary material available at https://doi.org/10.1186/s40317-023-00350-1.

Additional file 1: Figure S1. Unmanned surface vessel (USV) tracks (black line), stationary receivers (pink), and tag (green) location in the study area. Panels provide each run (1–8) with USV trials operated in station-keeping mode in the left column (trials 1, 4, and 7) and trials operated in drifting mode in the center and right columns (trials 2, 3, 5, 6, and 8). **Figure S2.** OPTION A. Temperature (°C) over time recorded at seven temperature loggers suspended within the water column near the line of stationary receivers in Hammond Bay, Lake Huron (45.5155, − 84.06943). Each line represents temperature recorded by a single logger, colored by height off bottom (m). Shaded regions indicate unmanned surface vessel (USV) trials with trial number given at the top (see Table 1 for trial descriptions). Heights off bottom notable to the study include: transmitter nearest to 8.3 m off bottom, USV receiver nearest to 21.35 m off bottom, stationary receivers nearest to 1.65 m off bottom. OPTION B. Temperature (°C) over time recorded at seven temperature loggers suspended within the water column near the line of stationary receivers in Hammond Bay, Lake Huron (45.5155, − 84.06943). Each line represents temperature recorded by a single logger, shown at the depth of the logger within the water column and colored by temperature (°C). Shaded regions indicate unmanned surface vessel (USV) trials with trial number given at the top (see Table 1 for trial descriptions). Dashed lines are labeled with the height of receivers and the transmitter used in the study (see methods for details).

Acknowledgements
We would like to thank John Thon for his help with the development of the CHASE USV, Zac Wickert (USGS) for field assistance, and Tim O'Brien (USGS) and Mark Dufour (USGS) for comments on the manuscript. Any use of trade, firm, or product names is for descriptive purposes only and does not imply endorsement by the U.S. Government.

Author contributions
XT, CH, and DH conceived the project. EG, XT, CH, TF, and DH conducted the experiments. TF conducted data analysis and modeling. EG and TF drafted the manuscript. All authors reviewed, edited, and approved the final manuscript.

Funding
The work was supported by the Great Lakes Fishery Commission (Grant 2022_TAN_441020).

Availability of data and materials
The data sets used and analyzed during the current study are available from the corresponding author upon request.

Declarations

Ethics approval and consent to participate
Not applicable.

Consent for publication
Not applicable.

Competing interests
The authors declare that they have no competing interests.

Received: 24 June 2023 Accepted: 25 October 2023
Published online: 22 November 2023

References

1. Matley JK, Klinard NV, Larocque SM, Weinz AA, Colborne SF. Space use of juvenile and subadult yellow perch (*Perca flavescens*) in the Detroit river using acoustic telemetry: incorporating variable detection ranges in vegetated areas. Can J Fish Aquat Sci. 2022;79(1):63–72.
2. Krueger CC, Holbrook CM, Binder TR, Vandergoot CS, Hayden TA, Hondorp DW, et al. Acoustic telemetry observation systems: challenges encountered and overcome in the Laurentian Great Lakes. Can J Fish Aquat Sci. 2018;75(10):1755–63.
3. Welch DW, Boehlert GW, Ward BR. POST–the Pacific Ocean salmon tracking project. Oceanol Acta. 2002;25(5):243–53.
4. Cooke SJ, Iverson SJ, Stokesbury MJW, Hinch SG, Fisk AT, VanderZwaag DL, et al. Ocean tracking network Canada: a network approach to addressing critical issues in fisheries and resource management with implications for ocean governance. Fisheries. 2011;36(12):583–92.
5. Binder TR, Farha SA, Thompson HT, Holbrook CM, Bergstedt RA, Riley SC, et al. Fine-scale acoustic telemetry reveals unexpected lake trout, Salvelinus Namaycush, spawning habitats in northern Lake Huron. North America Ecol Freshwater Fish. 2017;27(2):594–605.
6. Hussey NE, Kessel ST, Aarestrup K, Cooke SJ, Cowley PD, Fisk AT, et al. Aquatic animal telemetry: a panoramic window into the underwater world. Science. 2015. https://doi.org/10.1126/science.1255642.
7. Donaldson MR, Hinch SG, Suski CD, Fisk AT, Heupel MR, Cooke SJ. Making connections in aquatic ecosystems with acoustic telemetry monitoring. Front Ecol Environ. 2014;12(10):565–73.
8. Klinard NV, Halfyard EA, Matley JK, Fisk AT, Johnson TB. The influence of dynamic environmental interactions on detection efficiency of acoustic transmitters in a large, deep, freshwater lake. Anim Biotelemetry. 2019. https://doi.org/10.1186/s40317-019-0179-1.
9. Hayden TA, Holbrook CM, Binder TR, Dettmers JM, Cooke SJ, Vandergoot CS, et al. Probability of acoustic transmitter detections by receiver lines in Lake Huron: results of multi-year field tests and simulations. Anim Biotelemetry. 2016. https://doi.org/10.1186/s40317-016-0112-9.
10. Heupel MR, Semmens JM, Hobday AJ. Automated acoustic tracking of aquatic animals: scales, design and deployment of listening station arrays. Mar Freshw Res. 2006;57(1):1.
11. Kraus RT, Holbrook CM, Vandergoot CS, Stewart T, Faust MD, Watkinson DA, et al. Evaluation of acoustic telemetry grids for determining aquatic animal movement and survival. Methods Ecol Evol. 2018;9(6):1489–502.
12. Binder TR, Holbrook CM, Hayden TA, Krueger CC. Spatial and temporal variation in positioning probability of acoustic telemetry arrays: fine-scale variability and complex interactions. Anim Biotelemetry. 2016. https://doi.org/10.1186/s40317-016-0097-4.
13. Kuai Y, Klinard NV, Fisk AT, Johnson TB, Halfyard EA, Webber DM, et al. Strong thermal stratification reduces detection efficiency and range of acoustic telemetry in a large freshwater lake. Anim Biotelemetry. 2021. https://doi.org/10.1186/s40317-021-00270-y.
14. O'Brien MHP, Secor DH. Influence of thermal stratification and storms on acoustic telemetry detection efficiency: a year-long test in the US Southern Mid-Atlantic Bight. Anim Biotelemetry. 2021. https://doi.org/10.1186/s40317-021-00233-3.
15. Wells MG, Li J, Flood B, Kuai Y, Brooks JL, Cooke SJ, et al. Speed of sound gradients due to summer thermal stratification can reduce the detection range of acoustic fish tags: results from a field study in Hamilton Harbour, Ontario. Can J Fish Aquat Sci. 2021;78(3):269–85.
16. Oliver MJ, Breece MW, Haulsee DE, Cimino MA, Kohut J, Aragon D, et al. Factors affecting detection efficiency of mobile telemetry Slocum gliders. Anim Biotelemetry. 2017. https://doi.org/10.1186/s40317-017-0129-8.
17. Oliver MJ, Breece MW, Fox DA, Haulsee DE, Kohut J, Manderson JP, et al. Shrinking the haystack: using an AUV in an integrated ocean observatory to map Atlantic sturgeon in the coastal ocean. Fisheries. 2013;38(5):210–6.
18. Cimino M, Cassen M, Merrifield S, Terrill E. Detection efficiency of acoustic biotelemetry sensors on wave gliders. Anim Biotelemetry. 2018. https://doi.org/10.1186/s40317-018-0160-4.
19. Mordy CW, Cokelet ED, De Robertis A, Jenkins R, Kuhn CE, Lawrence-Slavas N, et al. Advances in ecosystem research Saildrone surveys of oceanography fish, and marine mammals in the Bering sea. Oceanography. 2017. https://doi.org/10.5670/oceanog.2017.230.
20. Hawkes LA, Exeter O, Henderson SM, Kerry C, Kukulya A, Rudd J, et al. Autonomous underwater videography and tracking of basking sharks. Anim Biotelemetry. 2020. https://doi.org/10.1186/s40317-020-00216-w.
21. Grothues TM, Dobarro J, Ladd J, Higgs A, Niezgoda G, Miller D. Use of a multi-sensored AUV to telemeter tagged Atlantic sturgeon and map

their spawning habitat in the Hudson River USA In IEEE/OES autonomous underwater vehicles. IEEE. 2008. https://doi.org/10.1109/AUV.2008.5347597.
22. Breece MW, Fox DA, Dunton KJ, Frisk MG, Jordaan A, Oliver MJ. Dynamic seascapes predict the marine occurrence of an endangered species: Atlantic sturgeon acipenser oxyrinchus oxyrinchus. Methods Ecol Evol. 2016;7(6):725–33.
23. Haulsee D, Breece M, Miller D, Wetherbee B, Fox D, Oliver M. Habitat selection of a coastal shark species estimated from an autonomous underwater vehicle. Mar Ecol Prog Ser. 2015;528:277–88.
24. Ennasr O, Holbrook CM, Hondorp DW, Krueger CC, Coleman D, Solanki PB, et al. Characterization of acoustic detection efficiency using a gliding robotic fish as a mobile receiver platform. Anim Biotelemetry. 2020. https://doi.org/10.1186/s40317-020-00219-7.
25. Zhang F, Tan X. Gliding robotic fish and its tail-enabled yaw motion stabilization using sliding mode control in of the dynamic systems and control. Am Soc Mechan Eng. 2014. https://doi.org/10.1115/DSCC2013-4015.
26. Zhang F, Wang J, Thon J, Thon C, Litchman E, Tan X. Gliding robotic fish for mobile sampling of aquatic environments. In: Proceedings of the 11th IEEE International Conference on Networking, Sensing and Control. IEEE; 2014.
27. Zhang F, Ennasr O, Tan X. Gliding robotic fish: an underwater sensing platform and its spiral-based tracking in 3D space. Mar Technol Soc J. 2017;51(5):71–8.
28. Zhang F, Ennasr O, Litchman E, Tan X. Autonomous sampling of water columns using gliding robotic fish: algorithms and harmful-algae-sampling experiments. IEEE Syst J. 2016;10(3):1271–81.
29. Shinzaki D, Gage C, Tang S, Moline M, Wolfe B, Lowe CG, et al. A multi-AUV system for cooperative tracking and following of leopard sharks. In: 2013 IEEE International Conference on Robotics and Automation. IEEE; 2013.
30. Webb DC, Simonetti PJ, Jones CP. SLOCUM: an underwater glider propelled by environmental energy. IEEE J Oceanic Eng. 2001. https://doi.org/10.1109/48972077.
31. Shanyfelt T, Joordens MA, Nagothu K, Jamshidi M. RF communication between surface and underwater robotic swarms. In: 2008 World Automation Congress. IEEE; 2008.
32. David Jeffrey Griffiths. Introduction to electrodynamics. Englewood Cliffs: Prentice-Hall; 1981.
33. Zuur AF, Ieno EN, Walker NJ, Saveliev AA, Smith GM. Mixed effects models and extensions in ecology with R. New York: Springer; 2011.
34. Wood SN. Fast stable restricted maximum likelihood and marginal likelihood estimation of semiparametric generalized linear models. J Royal Statist Soc Series B. 2010;73(1):3–36.
35. R Core Team. R: The R Project for Statistical Computing. R-project.org. 2023. https://www.r-project.org/.
36. Yoshida MA, Mabuchi K. Using a drifting GPS-Argos satellite buoy as a method for detecting acoustic-tagged fish offshore in an ancient lake. Anim Biotelemetry. 2023. https://doi.org/10.1186/s40317-023-00341-2.
37. Steel AE, Coates JH, Hearn AR, Klimley AP. Performance of an ultrasonic telemetry positioning system under varied environmental conditions. Anim Biotelemetry. 2014;2(1):15.
38. Kessel ST, Hussey NE, Webber DM, Gruber SH, Young JM, Smale MJ, et al. Close proximity detection interference with acoustic telemetry: the importance of considering tag power output in low ambient noise environments. Anim Biotelemetry. 2015. https://doi.org/10.1186/s40317-015-0023-1.
39. Scherrer SR, Rideout B, Giorli G, Nosal E, Weng KC. Depth—and range-dependent variation in the performance of aquatic telemetry systems: understanding and predicting the susceptibility of acoustic tag–receiver pairs to close proximity detection interference. PeerJ. 2018. https://doi.org/10.7717/peerj.4249.
40. Kessel ST, Cooke SJ, Heupel MR, Hussey NE, Simpfendorfer CA, Vagle S, et al. A review of detection range testing in aquatic passive acoustic telemetry studies. Rev Fish Biol Fisheries. 2013;24(1):199–218.
41. Carlson TL, Lindsey WJS, Chipps SR, Coulter AA, Schall BJ. Receiver mount design, transmitter depth, and wind speed affect detection probability of acoustic telemetry transmitters in a Missouri river tributary. Anim Biotelemetry. 2023. https://doi.org/10.1186/s40317-022-00313-y.
42. KMIMILLE10 Weather Station, Weather Underground, KMIMILLE10 (2022).

Publisher's Note